Numerical push-over analysis of a bridge piled foundation geotechnical and structural verification

Corigliano, Matteo; Flessati, Luca; Bongio, Piero; D'Angelantonio, Marco; di Prisco, Claudio Giulio

DOI
10.19199/2023.2.0557-1405.003

Publication date
2023

Document Version
Final published version

Published in
Rivista Italiana di Geotecnica

Numerical push-over analysis of a bridge piled foundation: geotechnical and structural verification

Matteo Corigliano*, Luca Flessati**, Piero Bongio***,
Marco D'Angelantonio***, Claudio Giulio di Prisco*

Summary

Most of the infrastructures in Europe are approaching their design life and, therefore, their safety under present conditions has to be reassessed. This is particularly crucial in the Italian context, since the current seismic design standards have significantly changed, being more severe than the previous ones. The goal of this paper is the critical evaluation of three different pseudo-static approaches for verifying at Ultimate Limit State a piled foundation of an existing bridge: (i) the standard one, neglecting the raft contribution and assuming foundation failure to be coincident with the failure of the most loaded pile, (ii) an analytical method, neglecting the raft contribution, but considering the ductile redistribution of forces on piles, (iii) a Finite Element numerical analysis, providing a push-over curve for the foundation system and considering both the raft-piles-soil coupling and the structural response of piles.

The results deriving from the first two approaches suggest the necessity of retrofitting measures for the case considered. In contrast, the more sophisticated numerical approach, providing a significant insight in the mechanical response of the system, puts in evidence that, under its current conditions, the foundation does not necessitate neither geotechnical nor structural retrofitting measures. More generally, this paper shows that considering the raft presence may allow a more rational and sustainable design of piled foundations.

1. Introduction

Most of the bridges in Italy and in Western countries have already reached their design life. For this reason, verifying whether these structures are still "safe", according to the current design standards, is very important, but individuating the most suitable retrofitting solution is sometimes very challenging. The retrofitting of foundations, in particular in case of pile groups, is very expensive and, in many cases, also technically difficult. In most of the cases, for tall bridges founded on piles, the most critical aspect is related to seismic actions and, in particular, to the moment capacity of the foundation [Anastasopoulos *et al.*, 2010]. According to the current design approaches [Eurocode 7, NTC2018], the contribution to bearing capacity of the raft is disregarded and the moment capacity is calculated by assuming the most loaded pile (under either tension or compression) to attain its axial bearing capacity.

* Dipartimento di Ingegneria Civile ed Ambientale, Politecnico di Milano
** Geoscience & Engineering Department, TUDelft
*** Tecne Gruppo Autostrade per l'Italia S.p.A

The design standards recognize the current practice to be over-conservative and the limit state to occur only when a significant number of piles fails together [Eurocode 7], but do not provide any calculation approach accounting the ductile redistribution of vertical forces on piles for. Only recently, an approach to estimate the bearing capacity of pile groups under vertical eccentric loads, accounting for the redistribution of forces due to the progressive achievement of the single pile bearing capacity, was proposed ([Di Laora *et al.*, 2019], [Iovino *et al.*, 2021]). Even in this case, the presence of the foundation raft is not considered and the loads transmitted by the superstructure are assumed to be carried out by piles only.

The role of the foundation raft and the coupled mechanisms involving the pile-raft-soil system are rarely analysed. From an experimental point of view, by performing centrifuge tests, [Sakellariadis and Anastasopoulos, 2022], have shown that the role of raft may be beneficial and not negligible. In the same paper, the authors confirmed, by performing non-linear piles-raft-soil interaction finite element (FE) numerical analyses, the experimental findings.

The goal of this paper is to put in evidence that FE numerical simulations can provide a significant insight in the mechanical response of piled founda-

 dx.doi.org/10.19199/2022.2.0557-1405.005

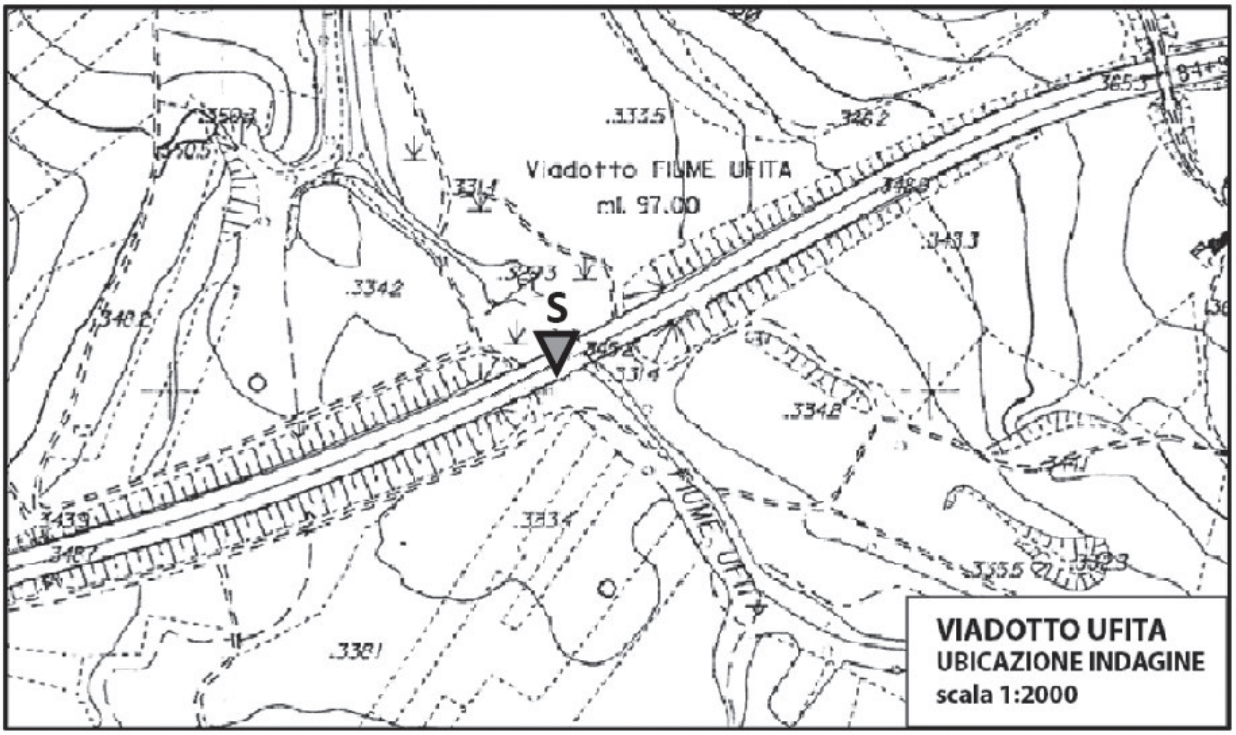

Fig. 1 – Investigation location.
Fig. 1 – Posizione del sondaggio.

tions, allowing to overcome some very overconservative assumptions on which simplified approaches, used in practice, are based on. This is expected to lead to a more aware design of new foundation systems and, in case of existing foundations, of retrofitting measures.

To this aim, a case study is analysed (§2). The pile group is verified under seismic actions by using a pseudo-static approach and by disregarding the kinematic interaction.

In §3 the foundation system is verified according to the current standards ([EC7] and [NTC2018]), that is by disregarding the raft and the ductile force redistribution on piles (§3.1). The verification (Geotechnical Verification 1, GV1) is performed by using the interaction domain defined in the M_y-V plane (the overturning moment and the vertical load transmitted by the superstructure, respectively). In §3.2 and §3.3 the approaches proposed by [DI LAORA *et al.*, 2019] and [DI LAORA *et al.*, 2022], are employed (GV2 and Structural Verification 2, SV2). The comparison in terms of interaction domains gives a quantitative information about the role of force redistribution for the foundation system taken into account. In §4 the authors illustrate the results of a non-linear 3D FE numerical simulation of the entire foundation system (piles + raft + soil), in terms of (i) synthetic push-over curves, defined as a function of overturning moment vs rotation angle and horizontal load vs horizontal displacements (Coupled Geotechnical Verification, CGV), (ii) plastic strains contours and (iii) internal actions in piles. In the numerical simulation, the structure response is assumed to be elastic. The structural failure (Coupled Structural Verification, CSV) is assumed, conservatively, to coincide with the first yielding in the most stressed pile cross-section.

Finally (§6), for the case study analysed, a critical comparison among the previously employed verification criteria is illustrated.

2. Case study

The Ufita viaduct, located in Southern Italy (Fig. 1), built at the end of the '70s, is 13m high and consists of three spans of 32m (Fig. 2) and a 18 m-wide deck. The piers are founded on rectangular piled rafts (Fig. 3) positioned in Ufita riverbed. The raft bases are at 4m depth from the ground surface, whereas the 7 reinforced concrete bored piles, connected to the raft, are 12 m long and with a diameter D = 1.2m. The reinforcement consists of 8 rebars with a diameter equal to 30mm and spiral stirrups.

(φ10/30cm). Recent restoration works gave occasion to a geotechnical characterization of the site. The soil profile was obtained by sampling the soil down to a depth of 25m close to the piled foundation base (red triangle S in Fig. 1 and Fig. 2). The soil profile (Fig. 4) is characterized by: (i) 1m of landfill material, (ii) 5 m of granular materials and

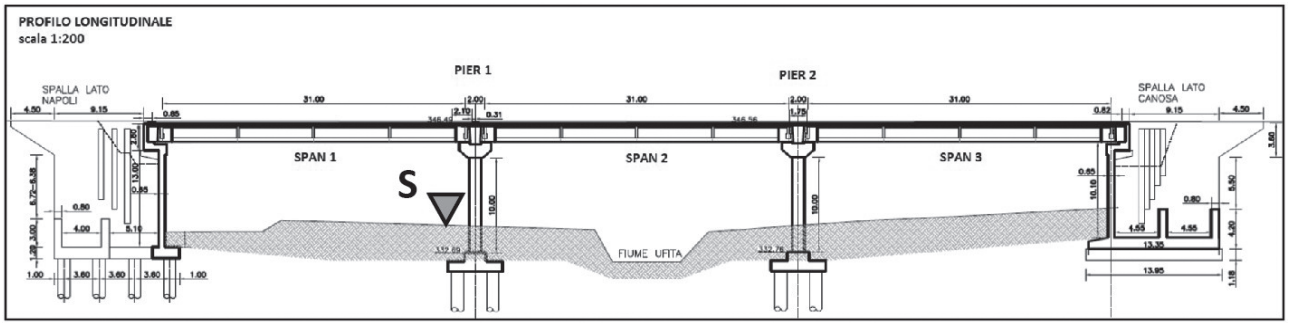

Fig. 2 – Longitudinal profile of the viaduct.
Fig. 2 – Sezione longitudinale del viadotto.

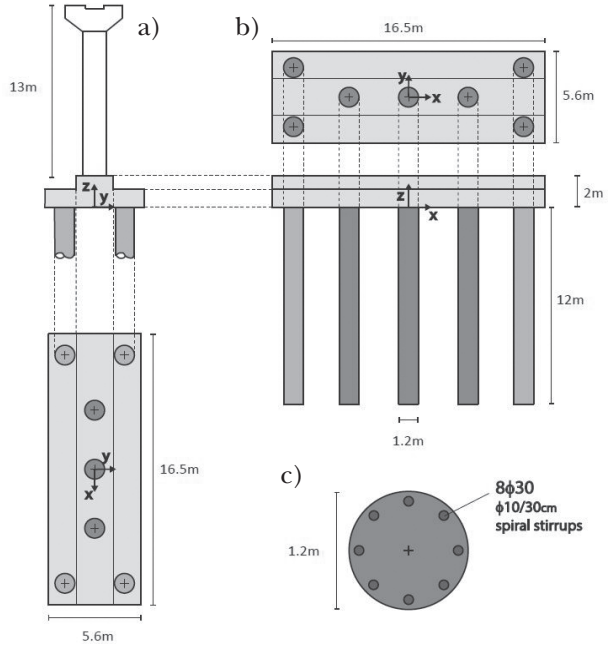

Fig. 3 – Geometry of the piled raft foundation: a) transversal section; b) longitudinal section; c) cross section of the single pile.
Fig. 3 – Geometria della fondazione su pali: a) sezione trasversale; b) sezione longitudinale; c) sezione del singolo palo.

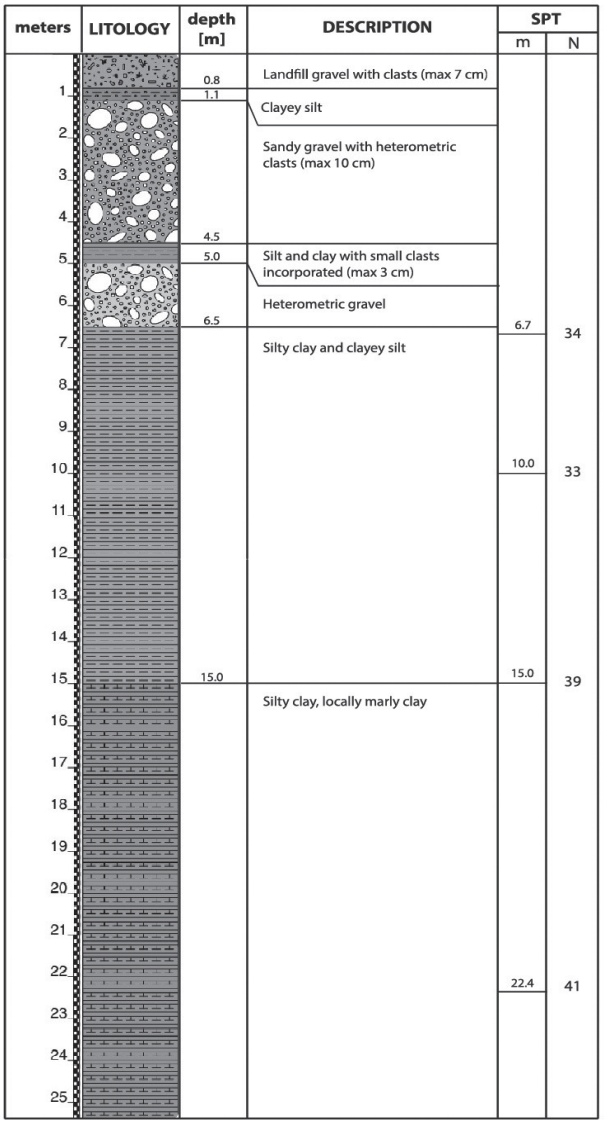

Fig. 4 – Soil profile and SPT tests.
Fig. 4 – Profilo del suolo e risultati del test SPT.

(iii) an underlying layer composed of fine-grained materials (clayey silt, silty and marly clay). In the boring hole a series of standard penetration tests (SPT) were performed. The results (Fig. 5a) were interpreted by means of the empirical Stroud correlation [STROUD, 1974] between the number of SPT blows and the undrained strength (S_u). The obtained S_u values (Fig. 5b) are practically constant along depth.

2.1. Engineering modelling of the foundation

To provide a safe side estimation of the bearing capacity of the foundation system, the granular material stratum is disregarded and the foundation system is assumed to be positioned in a saturated homogeneous clay soil stratum of unit weight equal to $\gamma_{sat} = 20\ kN/m^3$ As was previously mentioned, the verification of the foundation under seismic actions is

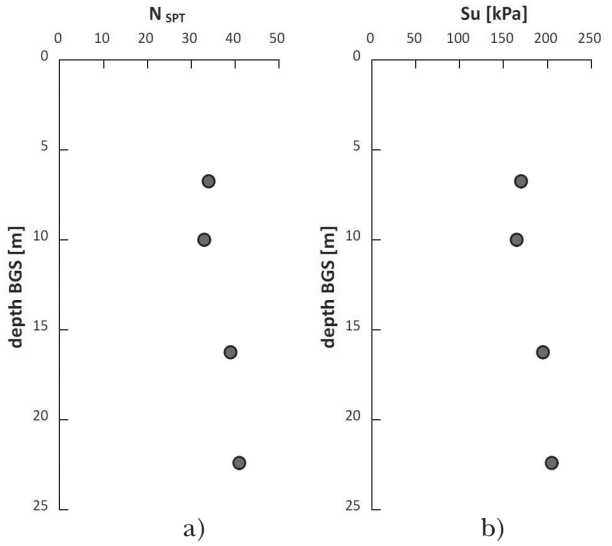

Fig. 5 – a) NSPT and b) undrained shear strength soil profiles.

Fig. 5 – a) profilo di NSPT e b) di resistenza non drenata lungo la profondità.

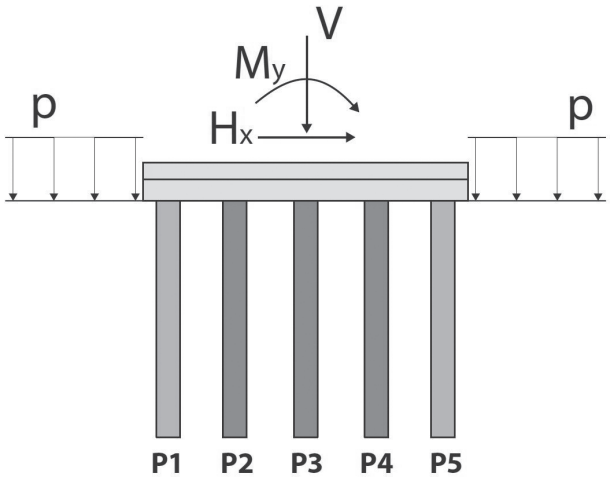

Fig. 6 – Geometrical scheme (longitudinal section) with applied loads.

Fig. 6 – Schema geometrico (sezione longitudinale) con carichi applicati.

performed by using a pseudo-static approach and by neglecting the kinematic interaction.

According to [NTC2018], under seismic actions, the foundation soil is assumed to behave under undrained conditions and to be characterized by a constant S_u along depth (z). To calculate the actions transmitted by the superstructure to the foundation, an uncoupled approach was used: the structural dynamic analysis for the viaduct was carried out, on the safe side [CONTI *et al.*, 2020], by assuming the soil to provide a rigid constraint to the structure.

Here below, for the sake of brevity, all the analyses will concern the foundation of pier number 1 of figure 2 and not all the foundations. The loads, all referred to the raft base centre, transmitted by the superstructure to this foundation are summarized in Table I, where V_d (including raft and backfill soil weight), $H_{x\,d}$, $H_{y\,d}$, stand for vertical, horizontal, along x and y respectively loads, whereas $M_{x\,d}$, $M_{y\,d}$ and $M_{z\,d}$, for the overturning moment around x, y and z (torque moment). Since $M_{x\,d}$, $M_{z\,d}$ and $H_{y\,d}$ are practically negligible, the foundation is verified for the sake of simplicity, by only considering V, M_y and H_x (Fig. 6), *i.e.* bending moment with axis coincident with the viaduct longitudinal axis, torque moment and horizontal load component along the orthogonal direction, are disregarded. As is schematized in Fig. 6, the lateral soil above the foundation level is, for the sake of simplicity, modelled as a uniform surcharge p, that is shear stresses mobilized along the lateral surfaces of both embedded raft and pier are neglected.

Tab I – Design loads under seismic actions.

Tab. I – Carichi di progetto in presenza di azione sismica.

V_d [kN]	$H_{x\,d}$ [kN]	$H_{y\,d}$ [kN]	$M_{x\,d}$ [kNm]	$M_{y\,d}$ [kNm]	$M_{z\,d}$ [kNm]
-28881	3810	873	8296	47946	265

3. Definition of the interaction domain according to simplified geotechnical/structural approaches

As is commonly done in the literature, in this section, the bearing capacity of piled foundations is calculated by assuming: (i) the raft to be rigid and not to transmit stresses to the soil, (ii) the soil at the interface with pile shaft and under the pile tip to be characterized by a rigid-perfectly plastic mechanical behaviour, (iii) pile heads to be rigidly connected with the raft by means of hinges (piles are only axially loaded) and (iv) the ultimate loads for each pile along horizontal and vertical directions to be independent to each other (the reduction in bearing capacity due to V-H_x coupling is disregarded).

In particular, in §3.1 the foundation system is verified according to [NTC2018], whereas in §3.2 according to the approach proposed by [DI LAORA, 2019]. Finally, in §3.3, the approach proposed by [DI LAORA, 2022] is employed.

3.1. Bearing capacity verification according to [NTC2018] (Geotechnical Verification 1 - GV1)

In this section, the interaction domain of the foundation system in the M_y-V plane is obtained by assuming the piles to be rigid and by accounting for the single axial load transmitted by each pile, when

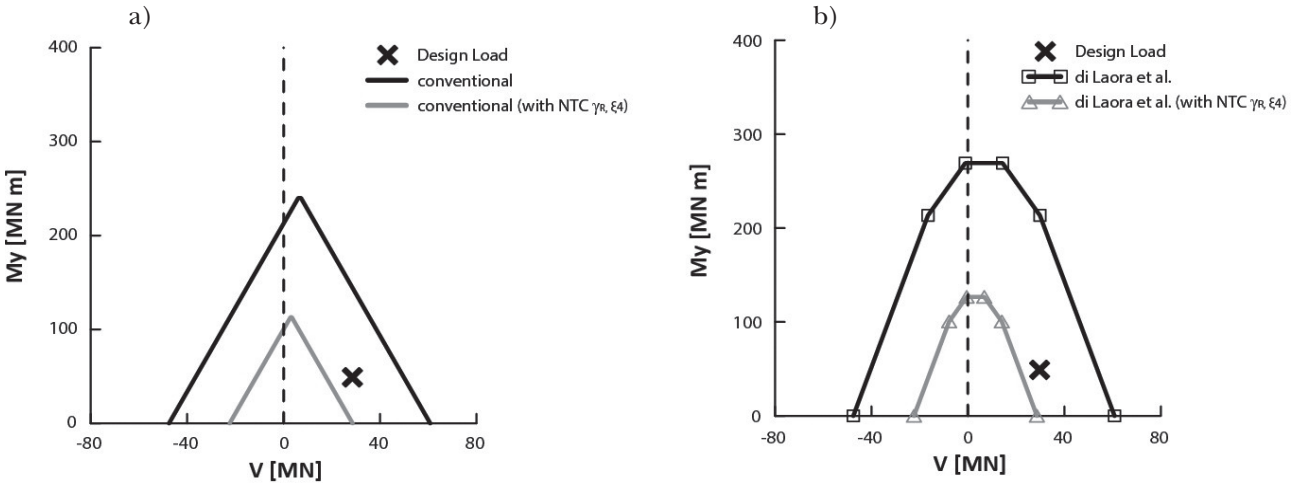

Fig. 7 – My-V interaction domains: (a) geotechnical failure of the first pile (GV1) and (b) geotechnical failure of the pile group (GV2).

Fig. 7 – Diagrammi di interazione nel piano My-V: (a) rottura geotecnica del primo palo (GV1) and (b) rottura geotecnica del gruppo di tutti i pali (GV2).

the most loaded pile gets its ultimate condition either under tension (Q_t) or compression (Q_s). According to the hypotheses introduced:

$$Q_T = Q_S = \pi D \mathrm{L} \alpha \mathrm{S_u} \quad (1)$$

$$Q_C = Q_S + Q_b = \pi D \mathrm{L} \alpha \mathrm{S_u} + (S_u N_C + \gamma_{sat} \mathrm{L} + p) \frac{\pi D^2}{4} \quad (2)$$

being Q_S the pile shaft resistance, Q_B the pile base resistance, $N_c = 9$ [Viggiani, 2012] and α=1. To account for the disturbance induced by the construction process, in the design phase α is commonly assumed to be lower than one [Viggiani, 2012]. In the present case, in contrast with what reasonably assumed for new constructions, the material close to the pile consolidated under the permanent loads coming from the viaduct and, therefore, the S_u value is larger than that measured externally.

By imposing a linear distribution for the vertical loads transmitted to piles (Q_i) and by imposing vertical balance of momentum and rotational equilibrium, the interaction domain in the M_y-V plane is obtained (Fig. 7a). In particular, the black curve is obtained without imposing the partial factors of safety, whereas the grey one by imposing factors of safety according to [NTC2018]: in this case Q_S is reduced by $\xi_4 = 1.7$ and γ_R (γ_R =1.25 for piles under tension and γ_R =1.15 for compressed piles) while Q_B is reduced by $\xi_4 = 1.7$ and γ_R =1.35. As is evident, the black cross in figure 7a, representing the design loads applied on the foundation system, lies outside the admissible envelope.

The interaction domain in the M_y-H_x-V space is illustrated in figure 8. In this figure, the maximum value of H_x is calculated by adding the contribution of each pile. This is evaluated according to [Broms, 1964], by assuming a fixed-head and an infinite value of the resistant bending moment (M_P) for the pile cross-section. This simplifying hypothesis does not affect the results of the verification, since for any H_x value, the foundation system is not verified (Fig. 7a).

3.2. Accounting for pile group ductile redistribution (Geotechnical Verification 2 - GV2)

In this section the piled foundation system is verified at ULS by employing the same design approach of [NTC2018] and by calculating the bearing capacity of the group according to what proposed by [Di Laora *et al.*, 2019], who suggested to account for the ductile redistribution of axial forces in the pile group. In this case, the axial forces transmitted to the piles follow a distribution characterized by a constant value where the piles get the ultimate axial load (Q_i equal either to Q_c or Q_T) and a linearly varying distribution where $Q_T < Q_i < Q_C$. By imposing vertical balance of momentum and rotational equilibrium, the interaction domain in the M_y-V plane is obtained (Fig. 7b). In particular, the black curve is obtained without applying the partial factors of safety, whereas the grey one by employing the same factors of safety of §3.1. As is evident, the black cross in figure 7b, representing the design loads applied on the foundation system, still lies outside the admissible envelope. This implies that, once again, the foundation is not verified. In this case, the difference between the interaction domains plotted in figure 7aa and figure 7b Fig. 7a and Fig. 7b is slight, due to the adopted geometrical configuration of piles. For the sake of brevity,

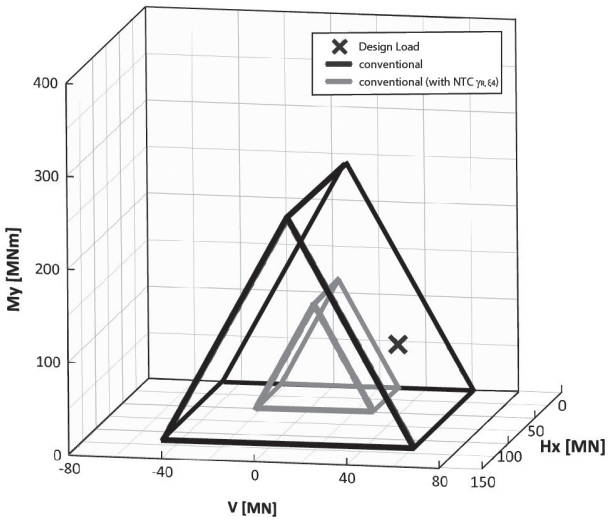

Fig. 8 – Interaction domain in My-Hx-V according to GV1.
Fig. 8 – Dominio di interazione nello spazio My-Hx-V seguendo l'approccio GV1.

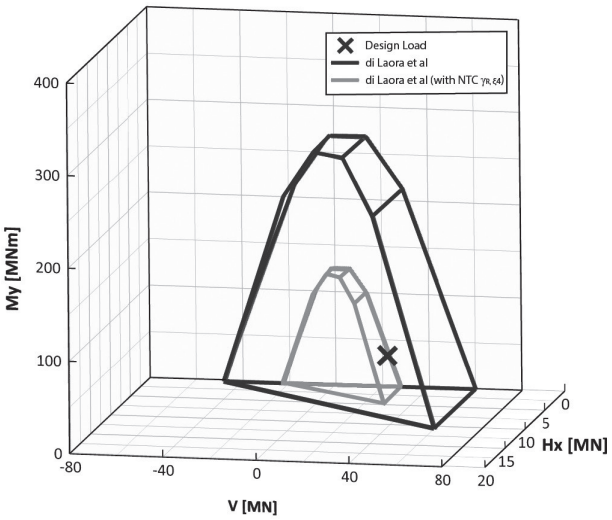

Fig. 9 – Interaction domain in My-Hx-V according to SV2.
Fig. 9 – Dominio di interazione nello spazio My-Hx-V seguendo l'approccio SV2.

the three-dimensional representation of the interaction domain is here omitted, since the foundation system verification is not satisfied even in case H_x=0.

3.3. Accounting for pile group ductile redistribution and pile structural failure (Structural Verification - SV2)

In this section, the authors employed the approach proposed by [DI LAORA *et al.*, 2022], assuming that the foundation interaction domain in the V-H_x –M_y space is determined (i) by following the Broms' approach [BROMS, 1964], (ii) by assuming the axial force acting in each pile i ($N_{PILE\ i}$) to be constant along depth, and (iii) in case $N_{PILE\ i}$ larger than the tensile resistance of the pile cross-section, $H_{x\ PILE\ i}$ = 0. Hypotheses (ii) and (iii) allow to calculate, by using the well-known $M_{P\ i}$ ($N_{PILE\ i}$) interaction domain, for each pile, independently of z and for each pile cross-section, the yield bending moment $M_{p\ i}$. Once $M_{P\ i}$ are assessed, the maximum $H_{x\ i}$ values can be calculated and H_x is obtained by adding all the single pile contributions $H_{x\ i}$. In figure 9 Ithe obtained foundation interaction domain is plotted.

Even in this case, the foundation is not verified.

4. Accounting for piles-raft-soil interaction (Coupled Geotechnical Verification - CGV) and structural failure (Coupled Structural Verification - CSV)

In this section, the authors illustrate the results of a non-linear 3D FE numerical analysis performed by using the commercial code MIDAS/GTS-NX and aimed at simulating the piles-raft-soil mechanical interaction. The geometry of the FE model, representing only one half of the domain (due to symmetry), is reported in figure 10. Model dimensions are chosen to avoid boundary effects. The numerical results, demonstrating the suitability of the chosen dimensions for the numerical model, are omitted for the sake of brevity.

The 3D soil domain has been discretized by means of about 92000 elements. The mesh is mainly composed of 6-node hexahedral elements but, where necessary, for geometrical reasons, also 5-node and 6-node pentahedrons are employed. Conversely to what done by [COMODROMOS *et al.*, 2016], both piles and raft are discretised by using solid elements. The mesh is more refined where higher strains are expected, *i.e.*, in proximity of piles and raft. The results demonstrating the suitability of the mesh employed are here omitted for the sake of brevity.

Piles and concrete raft (with a unit weight of 25 kN/m^3) are assumed to be elastic with a Young modulus of 30 GPa and a Poisson ratio equal to 0.3 (the results of a sensitivity analysis on this parameter performed by the authors allow to state that the numerical results do not differ if ν is ranging between 0.15 and 0.35).

As is illustrated here below, the initial state of stress and the vertical permanent loads are applied under drained conditions, by using an elastic perfectly plastic constitutive relationship with a Mohr-Coulomb failure criterion (friction angle ϕ'=20° cohesion c'= 0kPa, dilatancy angle ψ'=3°, Young modulus of 43 MPa and Poisson ratio 0.3).

The equivalent seismic loads are applied by assuming the soil to behave under undrained conditions and is modelled as a 1-phase elastic perfectly

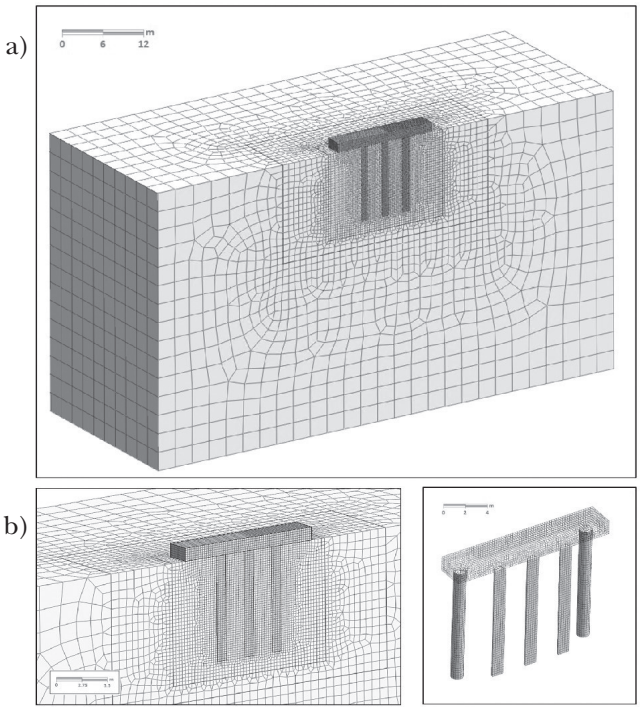

Fig. 10 – Finite element discretization for 3D numerical analyses: a) full model; b) zoom around the raft; c) zoom on the piled raft only.
Fig. 10 – Discretizzazione ad elementi finiti per l'analisi numerica 3D: a) intero modello; b) ingrandimento attorno alla platea; c) ingrandimento sulla palificata.

plastic material. Soil failure is reproduced by means of a Tresca criterion and the flow rule is assumed to be associated. Both S_u and elastic soil properties (assessed by using standard empirical correlations between material undrained stiffness and over consolidation ratio) are assumed to be constant along depth (S_u = 150kPa, undrained stiffness E_u=50*MPa* and Poisson ratio ν=0.5).

Elastic perfectly plastic interface elements have been set at both soil-pile and soil-raft interfaces. Along the normal direction, these elements are "quasi-rigid" under compression and perfectly fragile under tension (when detachment occurs both normal and tangential stresses become nil: the reduction in ultimate resistance due to pile soil separation is implicitly taken into account). Along the tangential direction, a nil dilatancy Tresca failure criterion is adopted (the limit tangential stress is imposed equal to S_u).

Both vertical and horizontal displacements are constrained at the bottom boundary. Along the lateral sides only vertical displacements are allowed.

The FE analysis has been carried out according to the following five distinct stages:

(i) imposition under drained conditions of the initial state of stress in the foundation soil before piled raft construction: the initial state of stress is obtained by progressively increasing gravity to the final unit weight value. During this phase the pile domain is assumed to be filled by soil elements.
(ii) drained pile construction: mechanical properties and unit weight in the pile domain are progressively changed.
(iii) drained raft construction.
(iv) progressive imposition under drained conditions of V: linear stepwise application of the vertical load on the raft due to the superstructure self-weight (load path P-Q in Fig. 11), up to the final vertical load design (V_d) value.
(v) imposition of M_y and H_x, under undrained conditions to simulate, according to the pseudo-static approach, the seismic inertial actions transmitted by the super-structure: both M_y and H_x are simultaneously increased (push-over test) up to failure (load path Q-S in Fig. 11). The ratio M_y/H_x is kept constant and equal to the ratio M_d/H_d.

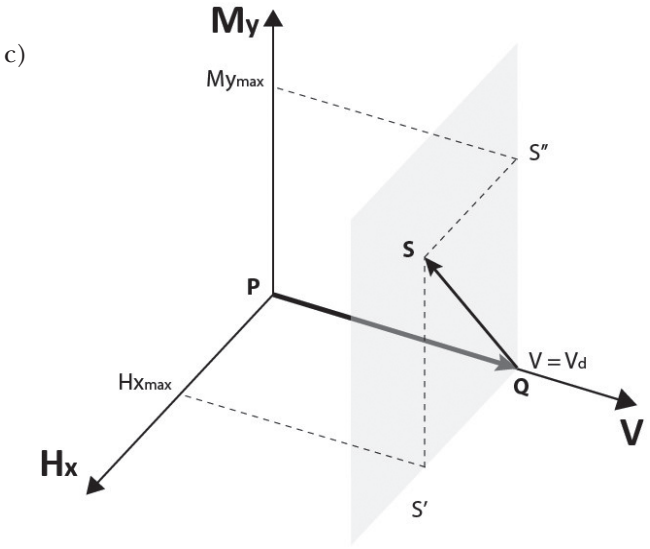

Fig. 11 – Load path in V-H_x-M_y space.
Fig. 11 – Percorso di carico nello spazio V-H_x-M_y .

4.1. FE Model results: the push-over curves

The numerical results relative to phase (v) are summarized in figure 12 in terms of M_y – θ curve, where θ is the raft rotation (Fig. 12a) and H_x – u curve, where u is the displacement along x direction (Fig. 12b). The foundation response is non-linear and both curves (Fig. 12a and b) are characterized by a final horizontal asymptote, corresponding to the limit load of the system, when a plastic mechanism develops in the soil domain.

To better understand the evolution of the plastic mechanism developing in the soil domain, deviatoric irreversible strain fields are illustrated in figure

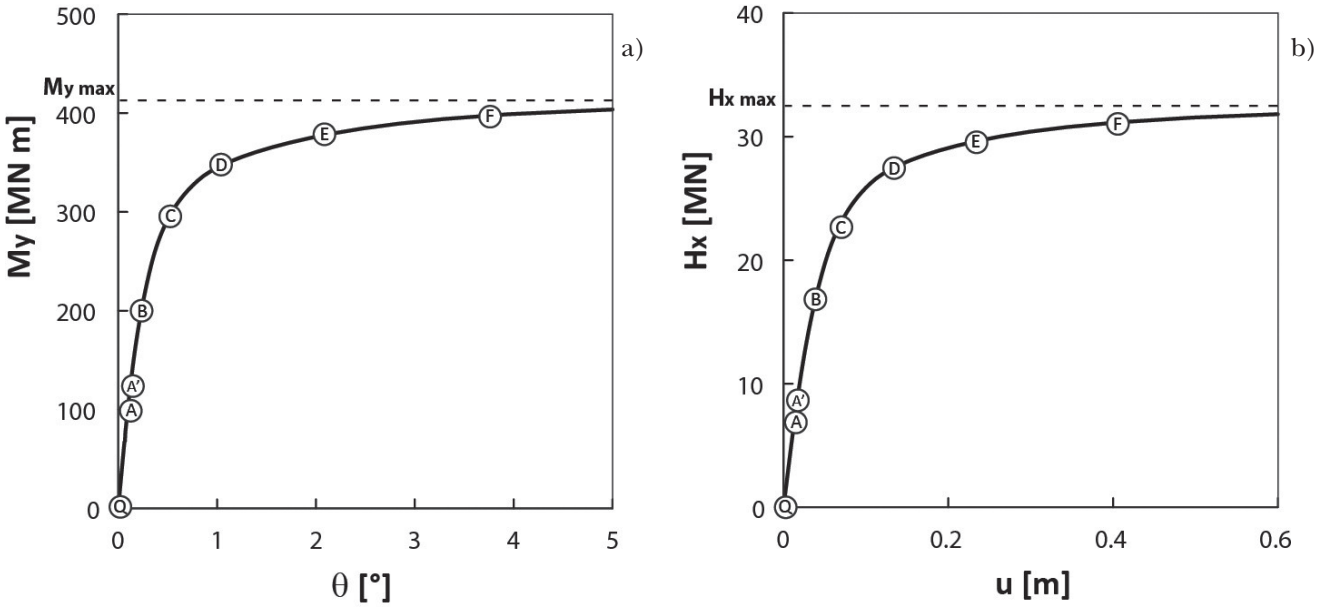

Fig. 12 – Undrained foundation response to combined loading: (a) Moment - rotation; (b) Horizontal load – horizontal translation.

Fig. 12 – Risposta non drenata della fondazione soggetta a carico combinato: (a) Momento – rotazione; (b) Carico orizzontale – traslazione orizzontale.

13 In particular, figure 13 a-f, f correspond to A-F points of figure 12 (point A' of Fig. 12 will be commented in §5).

Up to point B of figure 12, plastic strains are very small and mainly accumulate at the edge of the raft (Fig. 13a-b). Subsequently, when the system response becomes highly non-linear (point C of Fig. 12), the yielded domain, close to the raft edge, propagates downwards and plastic strains develop at the tip of the compressed piles (Fig. 13c). By further increasing the loads (points D and E of Fig. 12), the plastic mechanism, evolving from the raft edge, reaches compressed pile tips (Fig. 13d-e). At the same time yielding also take place around piles shaft and close to the left raft edge. Finally (point F of Fig. 12), the plastic mechanism closes and ge-

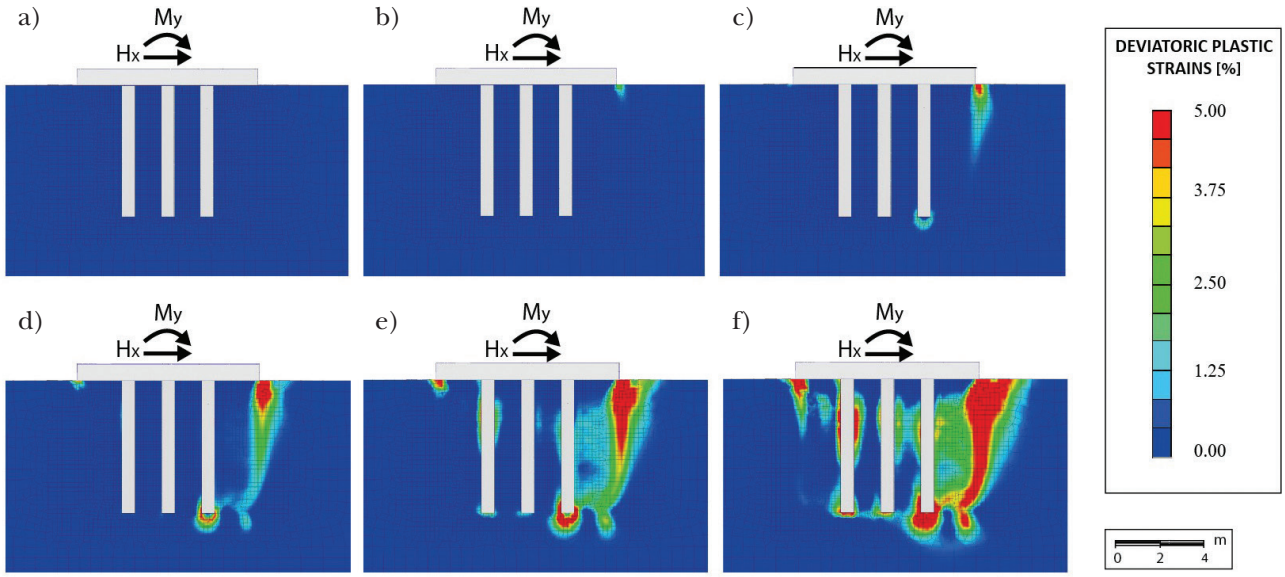

Fig. 13 – Evolution of plastic strain field in the soil around the piled foundation (a, b, c, d, e, f correspond to A, B, C, D, E, F points represented in Fig. 12).

Fig. 13 – Evoluzione delle deformazioni plastiche nel terreno attorno alla fondazione su pali (a, b, c, d, e, f corrispondono ai punti A, B, C, D, E, F rappresentati in Fig. 12).

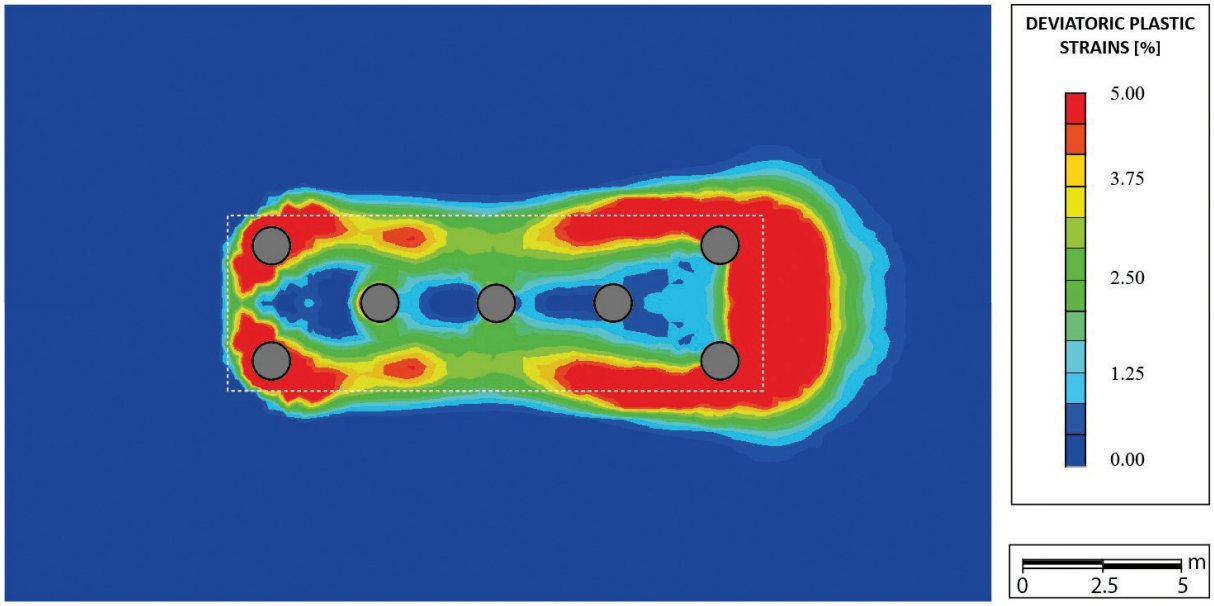

Fig. 14 – Plastic strain field in a cross-section at z=-2.5m at a load level correspondent to point F in Fig. 12.
Fig. 14 – Campo di deformazioni plastiche in una sezione a z=-2.5m per un livello di carico corrispondente al punto F in Fig. 12.

otechnical failure occurs for $M_y=M_{y\ max}$ and $H_x=H_{x\ max}$ (Fig. 12). It is worth mentioning that the observed failure mechanism is significantly different with respect to the one expected in case of shallow foundations: the presence of piles prevents the development of a shear failure mechanism in the soil close to the raft base.

To better describe the failure mechanism, a planar view of the irreversible deviatoric strains for a plane 2m deep under the foundation level (z = -2m), is reported in figure 14 .This figure testifies the role of the lateral piles, involved in the failure mechanism, and the absence of irreversibilities in the soil domain close to the central piles.

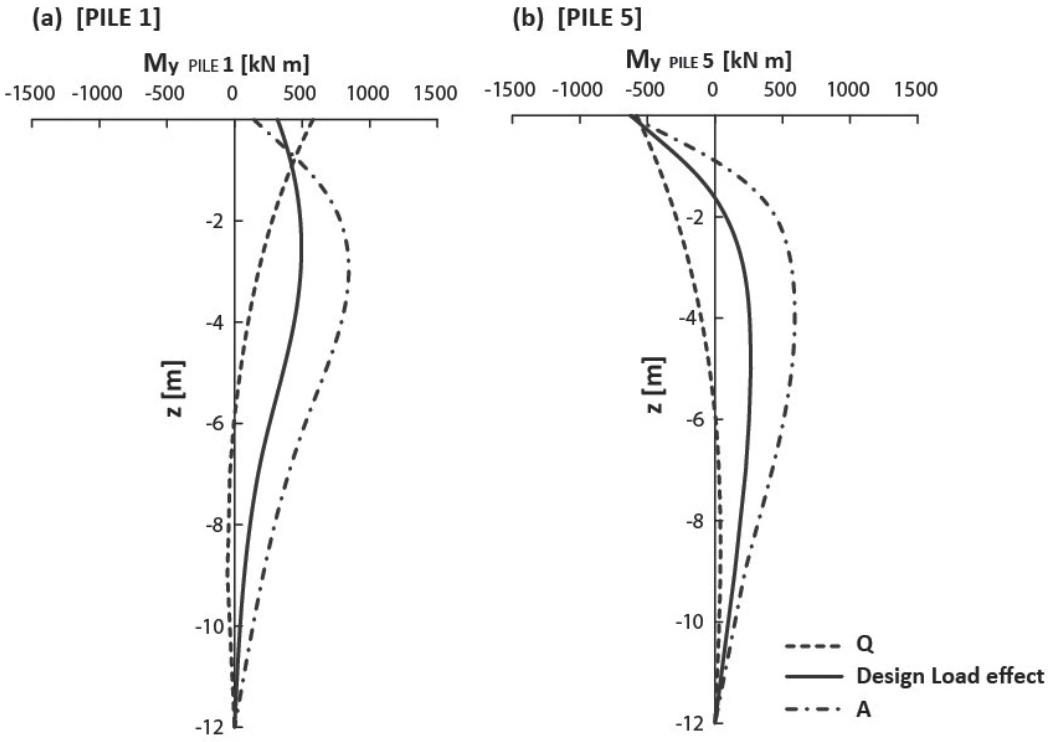

Fig. 15 – Evolution of M_{yPILE} for the most loaded piles (P1=P6 and P5=P7).
Fig. 15 – Evoluzione di M_{yPILE} per i pali più caricati (P1=P6 and P5=P7).

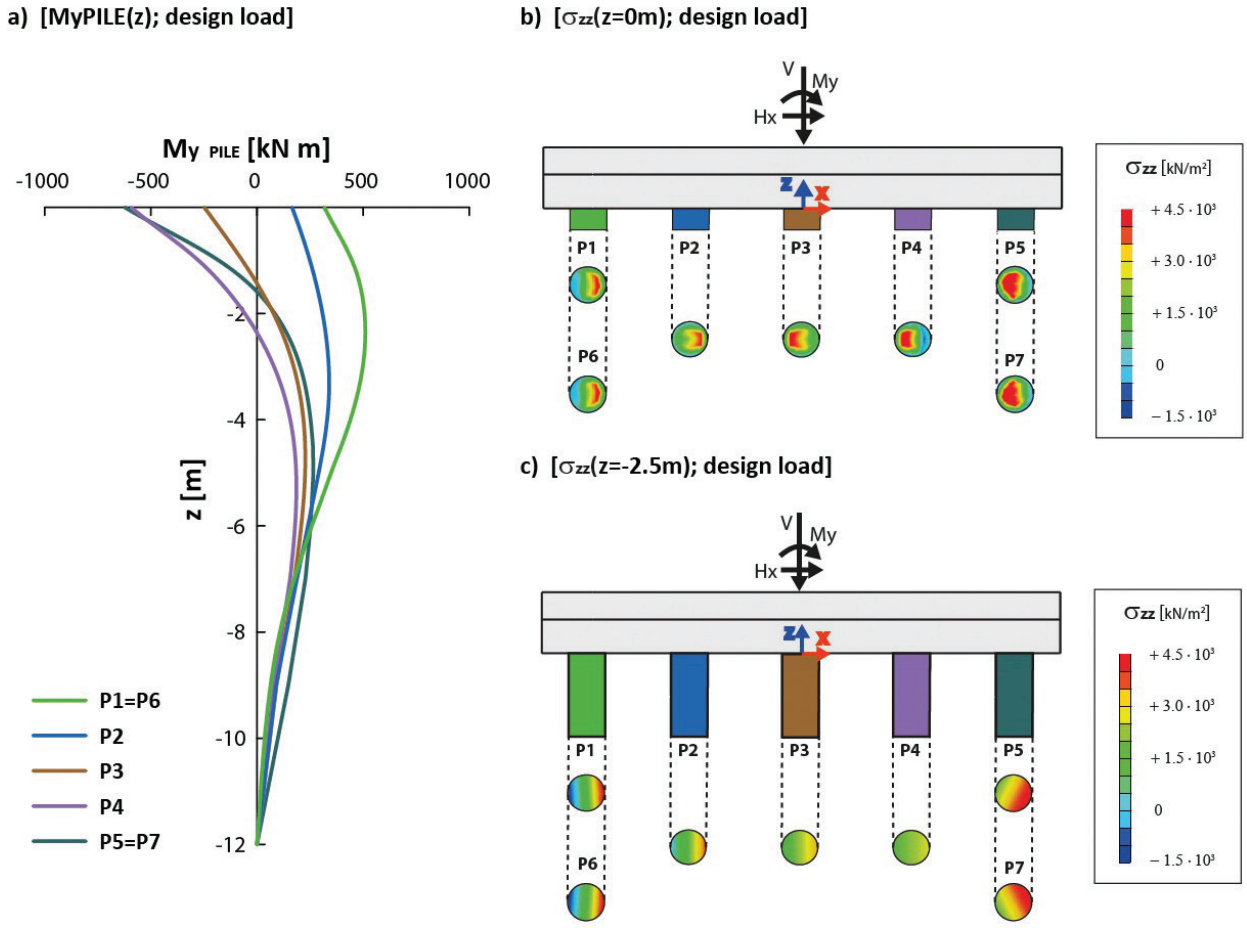

Fig. 16 – (a) M_{yPILE} along piles at design load (b) contours of vertical stresses in piles at pile head (c) contours of vertical stresses in piles at z=-2.5m (compression is assumed to be positive).

Fig 16 – (a) M_{yPILE} lungo i pali in corrispondenza del carico di progetto agente (b) campo di sforzi verticali alla testa dei pali (c) z=- campo di sforzi verticali a z=-2.5m (si assumono positivi gli sforzi di compressione).

4.2. Pile structural failure (Coupled Structural Verification - CSV)

As was previously mentioned, in the numerical FE model, both piles and raft are assumed to be elastic and rigidly connected to each other. In this section the authors analyze the structural response and, in particular, the authors want to verify the structural strength of the most loaded pile cross-section. To this aim, mandatory is the assessment of the bending moment, axial and shear loads along depth acting in each pile.

For the sake of brevity, here below the profiles along depth of $H_{x\ PILE\ i}$ (shear load along x acting in the single pile cross-section), $H_{y\ PILE\ i}$ (shear load along y acting in the single pile cross-section), $M_{y\ PILE\ i}$ (bending moment along x acting in the single pile cross-section) and $N_{PILE\ i}$, all evolving with the load applied on the raft foundation (M_y and H_x), are omitted.

In figure 15, the three profiles of $M_{y\ PILE}$ along depth (dashed, continuous, dot-dash, respectively) for piles P1 (Fig. 15a) and P5 (Fig. 15b) of Fig. 6 (the most loaded for any load condition taken into consideration) correspond to: (i) load level Q of figure 11,(ii) the design load and (iii) load level A of figure 12.

As is evident, under permanent loads (point Q of Fig. 11), $M_{y\ PILE\ 1}$ and $M_{y\ PILE\ 5}$ are, for the sake of symmetry, equal in modulus and opposite in sign (dashed lines). $M_{y\ PILE\ i}$ is not nil for any z value because of the deformability of the soil. $M_{y\ PILE\ i}$ is maximum at the pile head because of the raft stiffness.

When M_y and H_x are progressively increased, the bending moment distribution along depth evolves and the most loaded cross section (in terms of bending moment) goes downward.

In figure 16a, the seven $M_{y\ PILE\ i}$ vs z curves illustrate the distribution of bending moment in each pile for $H_{x\ d}$ and $M_{y\ d}$ (§2.1). As was expected, and this observation is valid for any H_x and M_y value, the most loaded piles are the two external ones (P1, P6 and P5, P7). In figure 16b and figure 16c Fig. 16b

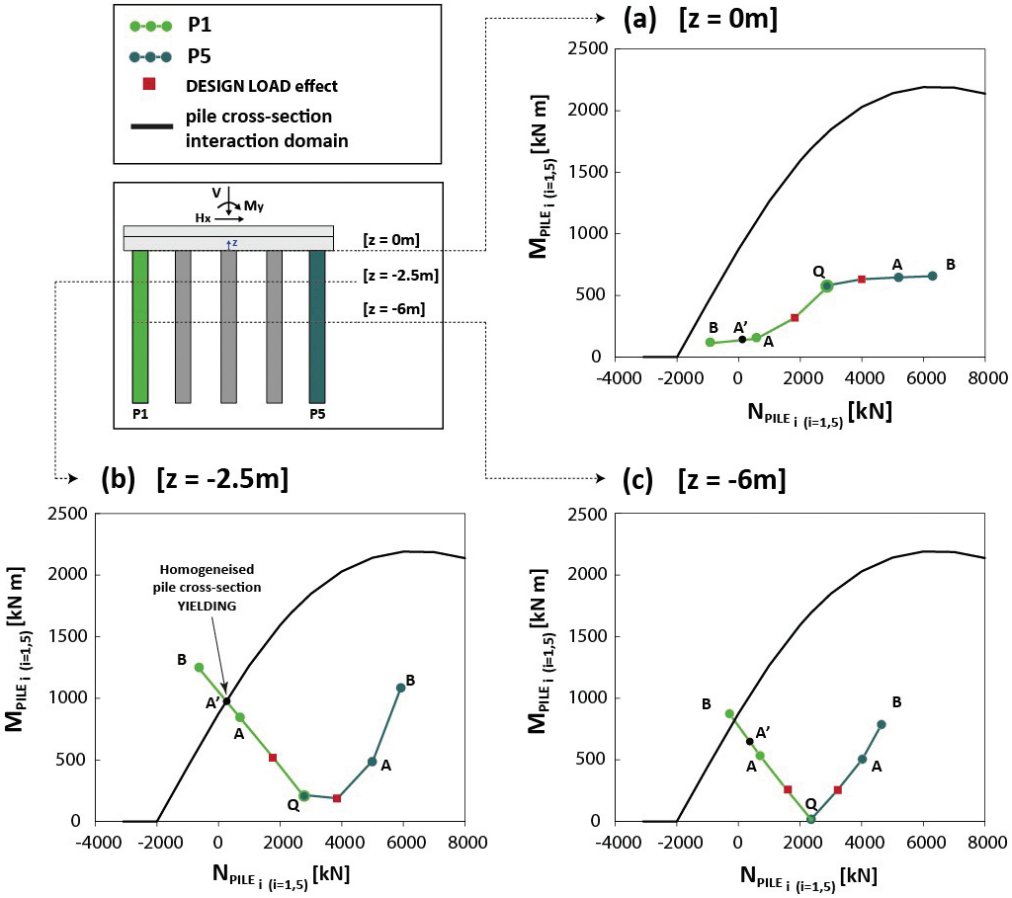

Fig. 17 – Generalized load paths for pile P1 and P5 at z=0m, z=-2.5m and z=-6m.
Fig. 17 – Percorsi di carico generalizzati per i pali P1 and P5 a z=0m, z=-2.5m e z=-6m.

and Fig. 16c the distribution of vertical stresses in the cross-sections corresponding to z = 0m and z = -2.5m are reported. As is evident, because of the soil presence, the $M_{y\ PILE\ i}$ is not the unique bending moment acting in the piles: $M_{x\ PILE\ i}$ is smaller but not negligible. In fact, the spatial distribution of normal stresses, in particular in piles P5 and P7 is not symmetric with respect to x axis.

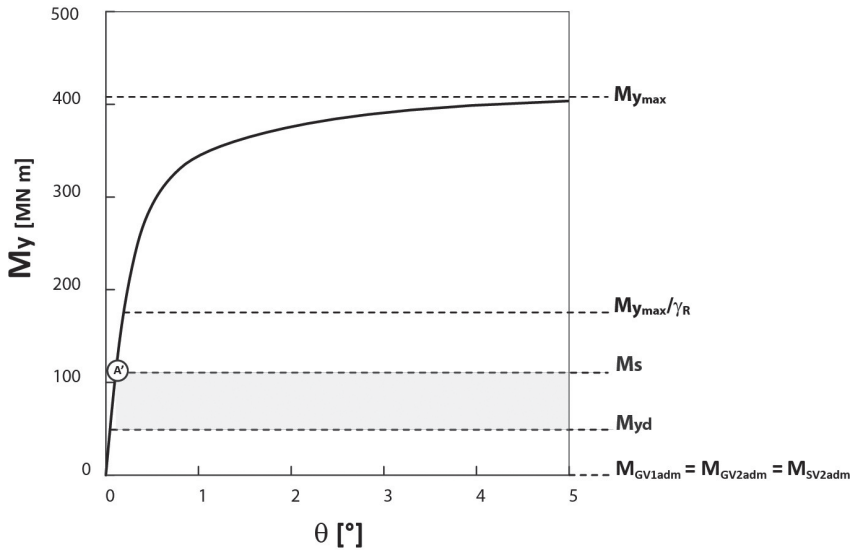

Fig. 18 – Summary and comparison of the results in M_y - θ plane.
Fig. 18 – Riassunto e confronto dei risultati nel piano M_y – θ.

With reference to piles P1 and P5 and cross sections positioned at z = 0m, z = -2.5m and z = -6m, in figure 17 the generalized stress paths, during phase (v), are plotted in terms of $M_{PILE\,i}$ and $N_{PILE\,i}$, where $M_{PILEi}(Z)=\sqrt{Mx^2_{PILEi}(Z)+My^2_{PILEi}(Z)}$. For the sake of clarity, in figure 17 generalized stress paths refer only to the beginning of the push-over curves (Q-B of Fig. 12). In the same figure, the black solid line represents the admissible domain of the reinforced concrete cross-section, determined by considering the design resistances for concrete f_{cd} =11.7 *MPa* and for steel f_{yd} =326*MPa*, respectively. The values of f_{cd} and f_{yd} were calculated by using (i) the strength values indicated in the original Ufita bridge design report (f_{ck} =20*MPa* and f_{yk} =375 *MPa* for concrete and steel, respectively) and (ii) [NTC2018] partial safety factors.

In point A' (Fig. 17b) of figure 12 (M_y=M_s), that is largely before the geotechnical failure, in pile P1, for z=-2.5m, the pile cross-section admissible domain is crossed for $N_{PILE\ 1}$ slightly larger than 0. In all the other piles and for any depth, the image-point A' lies inside the pile cross-section admissible M_{PILE}-N_{PILE} domain.

The authors have also verified the pile cross-sections under shear by comparing the shear internal actions calculated from the FEM numerical data with the pile cross-section structural shear resistance. According to this approach, the shear failure of the most critical cross-section takes place at the head of pile P1 for M_y=2.2M_d .

It is worth mentioning that the assumption of considering an elastic pile (neglecting the cracks developing in the concrete section [COMODROMOS *et al.*, 2009]) is on the safe side: by neglecting the reduction in stiffness associated with the formation of cracks in the most loaded pile provides an overestimation of the internal actions.

5. Critical discussion

In the previous sections, the piled raft foundation was verified under seismic actions by using three different pseudo-static approaches considering the inertial interaction and disregarding the kinematic one. In particular, the authors used: (i) the one suggested by [NTC2018], according to which bearing capacity is calculated by considering only the contribution of piles and by disregarding the ductile redistribution of forces in piles, (ii)-(iii) the ones suggested by [DI LAORA *et al.*, 2019; 2022], by considering only the contribution of piles, but not neglecting the ductile redistribution of forces, (iv) a numerical FE based approach, considering the raft-piles-soil coupling.

The results illustrated in the previous sections are summarized and compared in figure 18, where, for the sake of brevity, only the $M_y-\theta$ curve, obtained by performing the FE numerical analysis, is plotted. The five horizontal dashed lines correspond to:

(i) $M_{y\,d}$, (ii) M_{GV1adm} = M_{GV2adm} = M_{SV2adm} where M_{GV1adm} stands for the admissible M_y value obtained by using [NTC2018] (§3.1) while M_{GV2adm} and M_{SV2adm} , by using the [DI LAORA *et al.*, 2019; 2022] approaches, respectively (§3.2 and §3.2), (iii) Ms (§4.2) and (iv) $M_{y\,max}/\gamma_R$ (with γ_R equal to 2.3), (v) $M_{y\,max}$.

As is evident, $M_{y\,d}$ is smaller than M_s but larger than M_{GV1adm} , M_{GV2adm} and M_{SV2adm}. This implies that the more sophisticated approach, taking into consideration the raft presence, allows the verification of the foundation system without requiring any additional intervention of seismic risk mitigation.

Concluding remarks

The goal of this paper is to evaluate the bearing capacity of piled foundations of existing bridges. This topic is nowadays of great practical relevance since in Western countries many viaducts have reached their design life. The retrofitting of the foundations is very expensive and requires large investment in terms of time and raw materials. For these reasons, retrofitting measures have to be adopted only when necessary. In this paper, the authors analyze the case of an existing bridge and verify it at ULS by using four different approaches. The first three approaches are very simple, but, by disregarding the contribution of raft in evaluating the bearing capacity, they significantly underestimate the resistant resources of the foundation system. In contrast, the fourth approach, requiring the execution of a finite element numerical analysis, allows to both take the raft contribution into account and analyze the structural response of raft and piles. In the specific case taken into consideration, we can conclude that:

(i) according to the first three approaches, the foundation would need to be retrofitted;
(ii) in contrast, the more sophisticated displacement-based analysis seems to suggest that, under both permanent loads and seismic actions, the foundation has sufficient margin of safety from both geotechnical and structural perspective; not necessitating retrofitting measures.

It is evident that the use of more sophisticated calculation methods may lead to a more rational and sustainable foundation design.

Acknowledgment

This research is funded by Tecne Gruppo Autostrade per l'Italia S.p.A. within a research program aimed at defining innovative design solutions for the retrofitting of foundations of existing bridges.

References

ANASTASOPOULOS I., GAZETAS G., LOLI M., APOSTOLOU M., GEROLYMOS N. (2010a) – *Soil failure can be used for seismic protection of structures.* Bull. Earthquake Eng., 8, n. 2, pp. 309-326.

BROMS B. (1964) – *Lateral resistance of piles in cohesive soils.* Journal of the soil mechanics and foundations division, pp. 27-63.

COMODROMOS E.M., PAPADOPOULOU M.C., LALOUI L. (2016) – *Contribution to the design methodologies of piled raft foundations under combined loadings.* Canadian Geotechnical Journal, 53, n. 4, pp. 559-577.

COMODROMOS E.M., PAPADOPOULOU M.C., RENTZEPERIS I.K. (2009) – *The effect of cracking on the response of pile test under horizontal loading.* Journal of Geotechnical and Geoenvironmental Engineering, ASCE, Vol. 135, n. 9, pp. 1275-1284.

CONTI R., DI LAORA R., LICATA V., IOVINO M., DE SANCTIS L. (2020) – *Seismic performance of bridge piers: Caisson vs pile foundations.* Soil Dynamics and Earthquake Engineering, 130, 105985.

DI LAORA R., DE SANCTIS L., AVERSA S. (2019) – *Bearing capacity of pile groups under vertical eccentric load.* Acta Geotechnica, 14, n.1, pp. 193-205.

DI LAORA R., IODICE C., MANDOLINI A. (2022) – *A closed-form solution for the failure interaction diagrams of pile groups subjected to inclined eccentric load.* Acta Geotechnica, 17, pp. 3633-3646.

EN 1997-1 (2004) – *Eurocode 7: Geotechnical design - Part 1: General rules.* Authority: The European Union Per Regulation 305/2011, Directive 98/34/EC, Directive 2004/18/EC.

IOVINO M., MAIORANO R. M. S., DE SANCTIS L., AVERSA S. (2021) – *Failure envelopes of pile groups under inclined and eccentric load.* Géotechnique Letters, 11, n.4, pp. 247-253.

NORME TECNICHE PER LE COSTRUZIONI (NTC 2018). *Decreto ministeriale Ministero delle Infrastrutture e dei Trasporti (2018).*

SAKELLARIADIS L., ANASTASOPOULOS I. (2022) – *On the mechanisms governing the response of pile groups under combined VHM loading.* Géotechnique, in press.

STROUD M. A. (1974) – *The standard penetration test in insensitive clays and soft rock.* Proceedings of the 1st European Symposium on Penetration Testing, Sweden: Stockholm, 2, n. 2, pp. 367-375.

VIGGIANI C., MANDOLINI A., RUSSO, G. (2012). *Piles and pile foundations*, CRC Press.

Analisi negli spostamenti per la verifica geotecnica e strutturale di una palificata

Sommario

La gran parte delle infrastrutture europee sta raggiungendo la propria vita utile di progetto, pertanto la loro sicurezza nelle condizioni attuali deve essere nuovamente verificata. Nel contesto italiano questo aspetto è cruciale poiché le attuali normative sono significativamente cambiate e risultano essere più severe delle precedenti. L'obiettivo di questo lavoro è la valutazione critica di tre diversi approcci pseudo-statici per la verifica allo Stato Limite Ultimo di una fondazione su pali di un viadotto esistente: (i) l'approccio standard che trascura il contributo della platea e assume la rottura della palificata coincidente con la rottura del palo più sollecitato, (ii) un metodo analitico che trascura il contributo della platea ma considera la ridistribuzione duttile delle forze fra i pali, (iii) un approccio numerico agli elementi finiti, che fornisce una curva push-over per il sistema di fondazione e considera sia l'accoppiamento platea-pali-terreno che la risposta strutturale dei pali.

I risultati ottenuti utilizzando i primi due approcci sembrano suggerire la necessità, per il caso considerato, di mettere in opera interventi di adeguamento strutturale. Al contrario, i risultati ottenuti utilizzando l'approccio numerico più sofisticato indicano che, nelle condizioni attuali, la fondazione non necessita di interventi di rinforzo né dal punto di vista geotecnico né da quello strutturale. Più in generale, questo lavoro mostra che considerare la presenza della platea può consentire una progettazione più razionale e sostenibile delle fondazioni su pali.